ELSEVIER

Biochimica et Biophysica Acta 1367 (1998) 88–106

BIOCHIMICA ET BIOPHYSICA ACTA

BBA

Measurements of variable chlorophyll fluorescence using fast repetition rate techniques: defining methodology and experimental protocols

Zbigniew S. Kolber, Ondřej Prášil [1], Paul G. Falkowski *

Environmental Biophysics and Molecular Biology Program, Rutgers University, 71 Dudley Rd, New Brunswick, NJ 08901-8521, USA

Received 12 December 1997; revised 15 June 1998; accepted 23 June 1998

Abstract

We present a methodology, called fast repetition rate (FRR) fluorescence, that measures the functional absorption cross-section ($\sigma_{PS\,II}$) of Photosystem II (PS II), energy transfer between PS II units (p), photochemical and nonphotochemical quenching of chlorophyll fluorescence, and the kinetics of electron transfer on the acceptor side of PS II. The FRR fluorescence technique applies a sequence of subsaturating excitation pulses ('flashlets') at microsecond intervals to induce fluorescence transients. This approach is extremely flexible and allows the generation of both single-turnover (ST) and multiple-turnover (MT) flashes. Using a combination of ST and MT flashes, we investigated the effect of excitation protocols on the measured fluorescence parameters. The maximum fluorescence yield induced by an ST flash applied shortly (10 μs to 5 ms) following an MT flash increased to a level comparable to that of an MT flash, while the functional absorption cross-section decreased by about 40%. We interpret this phenomenon as evidence that an MT flash induces an increase in the fluorescence-rate constant, concomitant with a decrease in the photosynthetic-rate constant in PS II reaction centers. The simultaneous measurements of $\sigma_{PS\,II}$, p, and the kinetics of Q_A^- reoxidation, which can be derived only from a combination of ST and MT flash fluorescence transients, permits robust characterization of the processes of photosynthetic energy-conversion.

1. Introduction

Because its measurement is non-destructive, non-invasive, rapid, sensitive, and achieved in real-time [1], the change in the quantum yield of chlorophyll fluorescence induced by actinic light is used extensively to derive photosynthetic parameters related to PS II [2]. Theoretical and empirical models have

Abbreviations: $a_{PS\,II}$, optical cross section of PS II; Chl, chlorophyll; $C(t)$, fraction of closed PS II reaction centers at time t during FRR excitation protocol; $f(t)$, fluorescence yield at time t during FRR protocol; FRR, fast repetition rate; F_o, minimal fluorescence yield; F_m, maximal fluorescence yield; $g(t)$, function describing the kinetics of Q_A^- reoxidation; $g(t)=\alpha_1\exp(-t/\tau_1)+\alpha_2\exp(-t/\tau_2)+\alpha_3\exp(-t/\tau_3)$; HF1, F_m induced by first ST excitation in dark-adapted cells; HF2, F_m induced by ST flash applied following MT flash; HFM, F_m induced by MT excitation; $i(t)$, excitation intensity at time t in FRR protocol; $I(t)$, cumulative excitation energy in FRR protocol; LED, light-emitting diode; LF, F_m induced by ST excitation; MT, multiple turnover; p, extent of energy transfer between PS II reaction centers; PAM, pulse amplitude modulation fluorometry; P&P, pump-and-probe fluorometry; PQ, plastoquinone pool; PS II, Photosystem II; $q_p(t)$, photochemical quenching at time t during the FRR protocol; Q_A, the primary quinone electron acceptor in PS II; Q_B, the secondary quinone electron acceptor in PS II; $\sigma_{PS\,II}$, functional (i.e., the photochemically effective) cross section of PS II; RC II, reaction center of PS II; ST, single turnover; ST1, ST2, ST flashes applied before and after the MT flash, respectively

* Corresponding author. Fax: +1 732-932-8578; E-mail: falko@ahab.rutgers.edu

[1] Present address: Institute of Microbiology, MBU, AVČR, 379 81 Třeboň, Czech Republic.

0005-2728/98/$ – see front matter
PII: S0005-2728(98)00135-2

been proposed that relate variations in fluorescence yields to: (1) the quantum efficiency of photochemistry in PS II reaction centers [3–5]; (2) the number of primary and secondary electron-acceptors [6,7]; (3) the concentration of P^{+}_{680}, donor side turnover, and the state of the water-splitting system [8–10]; (4) the functional (or effective) absorption cross-section of PS II [11–16]; (5) energy transfer between reaction centers [17,18]; and (6) the kinetics of electron transport on the acceptor side of PS II [19–24]. These parameters provide information on the fundamental biophysical properties of photosynthetic energy conversion [25,26], the effects of environmental stresses on PS II function in vivo [27], photosynthetic electron transport under ambient irradiance [28], and the molecular relationships between the structure and function of the photosynthetic apparatus [29].

Experimentally, evaluating specific photosynthetic parameters partly depends upon the particular fluorometric method, instrument, and measurement protocol used. Consequently, comparing published results is complicated by differences in experimental techniques, and has led to contention about the validity and weaknesses of specific ones [14,18,30–34]. Confusion on the quantitative interpretation of variable fluorescence yields stems largely from differences between ST and MT excitation protocols [35–37].

The oldest, and easiest, technique for measuring changes in fluorescence yields is based on the analysis of a fluorescence transient induced in a dark-adapted sample by a short, rapid exposure to continuous light [38,39]. This so-called 'fluorescence induction technique' is beguilingly simple; however, because the rate of excitation delivery to PS II reaction centers (i.e., the rate of photochemistry) in a dark-adapted state is generally lower than the initial rate of Q_A^- oxidation, the observed transient saturates only after reduction of the plastoquinone pool [6]. As the stoichiometry of PQ to PS II is invariably >1.0 in vivo, the kinetics of the changes in fluorescence yields are complicated by multiple turnovers of PS II. This complication can be avoided by applying 3-(3,4-dichlorophenyl)-1,1-dimethylurea (DCMU) or similar herbicides that prevent reoxidation of Q_A^- on the relevant time scales of measurements. Use of such inhibitors, however, is not practical in in situ applications.

Subsequently, non-destructive ST and MT fluorescence-based techniques have been developed that expose samples to one or more flashes of saturating actinic light, and then follow changes in fluorescence as the electron acceptors in PS II are reduced. One widely used technique is the so-called 'light doubling' [40], or 'pulse amplitude modulated' (PAM method), that uses an MT actinic pulse to induce the maximum fluorescence level, as advocated by Shreiber [41]. An alternative to the MT approach is based on 'pump-and-probe' (P&P), or 'flash photolysis' techniques ([24,42–48]; see reviews in Refs. [39,48,49]). The P&P method compares fluorescence yields for weak probe flashes before and after an ST actinic 'pump' flash. Varying the intensity of the actinic flash allows the functional absorption cross-section of PS II to be derived [25] and, by varying the delay between actinic- and probe-flashes, the kinetics of electron transfer on the acceptor side of PS II also can be evaluated [23,24,50,51].

Both PAM and P&P techniques are superior to the fluorescence induction method because they permit more robust biophysical analyses; however, the required experimental protocols last up to several minutes, making it difficult to follow dynamic changes in the kinetics of electron transport and $\sigma_{PS\,II}$ occurring in time-scales of milliseconds to minutes. In addition, both techniques use excitation protocols that potentially change the redox state of electron carriers between PS II and PSI, and/or the level of nonphotochemical quenching within the photosynthetic apparatus. Consequently, the measured variable fluorescence critically depends upon the measurement protocol. Specifically, it was suggested that the P&P technique can induce so-called 'donor-side quenching' [8,10,43,52], whereas the PAM technique may mediate a different type of quenching resulting from excitation-induced changes in the redox state of the PQ pool [36,37,51].

Here we describe a novel methodology, called 'fast repetition rate' (FRR) fluorescence, that measures a suite of photosynthetic parameters, and examine how experimental protocols affect the measured quantum yields. Using this FRR approach, we can *independently* manipulate photochemical quenching, non-photochemical quenching, and the redox state of the acceptor and donor side of PS II, thereby assessing the contribution of each process to the variable fluorescence yield. Our goal is to extend the application

of fluorescence-based measurements of photosynthetic performance, while clarifying pragmatic issues of the applying experimental data to interpret the biophysical phenomena. In another paper, we examine the processes responsible for the variation in the quantum yields of fluorescence [53].

2. Materials and methods

2.1. Fast repetition rate fluorometry: theory

The FRR technique measures fluorescence transients induced by a series of brief subsaturating excitation pulses, or 'flashlets,' where the intensity, duration, and interval between them is independently controlled. This flexibility permits selective manipulation of Q_A and PQ reduction and allows changes in fluorescence yield to be separately attributed to the reduction states of these two acceptors. The FRR technique allows $\sigma_{PS\,II}$ and the energy transfer between PS II reaction centers to be calculated from the kinetics of fluorescence transients *within a single photochemical turnover* of PS II.

The fluorescence yield measured at time t during an FRR excitation protocol, $f(t)$, is defined by the F_o (minimal) and F_m (maximal) components of the fluorescence yield, and by the fraction of closed PS II reaction centers, $C(t)$. If the ensemble of PS II reaction centers share excitation energy [17,18,26,54], the observed fluorescence yield also depends on the extent of energy transfer, p:

$$f(t) = F_o + (F_m - F_o)\left(C(t)\frac{1-p}{1-C(t)p}\right). \quad (1)$$

Eq. 1 also can be expressed in terms of the fraction of open RC IIs, $q(t)=1-C(t)$, but at the cost of a more complicated formalism [26].

$C(t)$ is controlled by the rate of primary photochemistry, which is proportional to the product of incident excitation energy (I), the functional absorption cross-section ($\sigma_{PS\,II}$), and the rate of Q_A^- reoxidation. Changes in $C(t)$ due to primary photochemistry can be described as:

$$\frac{\partial C(t)}{\partial I} = \sigma_{PS\,II}\frac{1-C(t)}{1-C(t)p}. \quad (2)$$

Ignoring Q_A^- reoxidation (or assuming a single turnover character of the excitation), Eq. 2 simplifies to:

$$\frac{dC(t)}{dt} = \sigma_{PS\,II}\frac{dI\ 1-C(t)}{dt\,1-C(t)p} = \sigma_{PS\,II}\ i(t)\frac{1-C(t)}{1-C(t)p} \quad (3)$$

where $i(t)$ is the excitation intensity. Integrating Eq. 3 allows the expression of $C(t)$ as:

$$C(t) = \int_0^t \sigma_{PS\,II}\ i(\upsilon)\frac{1-C(\upsilon)}{1-C(\upsilon)p}d\upsilon, \quad (4)$$

where υ is the integration variable, and $C(\upsilon=0)$ is the fraction of PS II reaction centers closed before the FRR excitation. Substituting Eq. 4 into Eq. 1 allows calculation of the fluorescence transient, $f(t)$, when the rate of excitation delivery to RC II (i.e., the product of $i(t)$ and $\sigma_{PS\,II}$) greatly exceeds the rate of Q_A^- reoxidation. Such conditions exist at very high excitation intensities, or when Q_A^- reoxidation is inhibited by a herbicide, such as DCMU. In the more general case, where Q_A^- reoxidation is significant, Eq. 4 can be modified to account for this competing process:

$$C(t) = \int_0^t \sigma_{PS\,II}\ i(\upsilon)\frac{1-C(\upsilon)}{1-C(\upsilon)p}g(t-\upsilon)d\upsilon \quad (5)$$

where $g(t-\upsilon)$ describes the rate of Q_A^- reoxidation, expressed as a sum of exponential components:

$$g(t-\upsilon) = g(\Delta t) = \alpha_1\exp(-\Delta t/\tau_1) + \alpha_2\exp(-\Delta t/\tau_2) + \alpha_3\exp(-\Delta t/\tau_3). \quad (6)$$

Although there are no analytical solutions for Eqs. 4 and 5, the photosynthetic parameters (F_o, F_m, $\sigma_{PS\,II}$, p, as well as the kinetic constants in Eq. 6) can be calculated by numerically fitting the measured fluorescence transient to a discrete form of Eq. 1:

$$f_n = F_o + (F_m - F_o)C_n\frac{1-p}{1-C_n p} \quad (7)$$

where f_n is the fluorescence yield measured at the nth flashlet, and C_n is the fraction of RC II closed at the nth flashlet. C_n can be approximated recursively as:

$$C_n = C_{n-1}\sum_{k=1}^{m}A_{n,k} + I_n\sigma_{PS\,II}\frac{1-\left(C_{n-1}\sum_{k=1}^{m}A_{n,k}\right)}{1-p\left(C_{n-1}\sum_{k=1}^{m}A_{n,k}\right)} \quad (8)$$

where I_n is the excitation energy delivered at the nth flashlet, m is the number of exponential components in Eq. 6, and $A_{n,k}$ is determined by the kinetics of Q_A^- reoxidation:

$$A_{n,k} = (A_{n-1,k} + C_{n-1}\alpha_k/\sigma_{PS\,II})\exp(-\Delta t/\tau_k). \quad (9)$$

In practice, we assume that the kinetics of Q_A^- reoxidation (i.e., the amplitudes, α_k, and the time constants, τ_k, in Eq. 6 and Eq. 9) are constant during the excitation protocol. Q_A^- reoxidation can be calculated more rigorously by performing multiple numerical analyses for subsets of experimental data by individually evaluating α_k and τ_k while holding F_o, F_m, p, and $\sigma_{PS\,II}$ constant.

Ignoring Q_A^- reoxidation, Eq. 1 and Eq. 4 can be combined as follows:

$$C(t)=\sigma_{PS\,II}\int_0^t i(\upsilon)\frac{F_m-f(\upsilon)}{F_m-F_o}d\upsilon=\sigma_{PS\,II}\int_0^t [i(\upsilon)q_p(\upsilon)]d\upsilon, \quad (10)$$

where $q_p(t)=[F_m-f(t)]/[F_m-F_o]$ is the photochemical quenching. In absence of energy transfer (i.e., when $p=0$) $q_p=q=1-C$. The *functional* absorption cross-section for the photochemical target can therefore be calculated as:

$$\sigma_{PS\,II} = \left[\int_0^\infty [i(\upsilon)q_p(\upsilon)]d\upsilon\right]^{-1} \quad (11)$$

or, in discrete form:

$$\sigma_{PS\,II} = \left[\sum_{i=0}^{N}(I_n q_{p,n})\right]^{-1} \quad (12)$$

where N is the flashlet number at which the observed fluorescence signal saturates at the maximum level, F_m, and $q_{p,n}$ is the photochemical quenching measured during the nth flashlet. Eq. 12 gives an initial estimate of $\sigma_{PS\,II}$ for iteratively calculated photosynthetic parameters using Eqs. 7–9.

$\sigma_{PS\,II}$ describes the maximal efficiency of light utilization for photochemistry in PS II in units of Å^2/quanta:

$$\sigma_{PS\,II} = \frac{\partial C}{\partial I}|_{C=0} \quad (13)$$

$\sigma_{PS\,II}$ itself is controlled by light absorption and the quantum yield of photochemistry in the reaction centers:

$$\sigma_{PS\,II} = \frac{\partial E_a}{\partial I}\frac{\partial C}{\partial E_a}|_{C=0} = a_{PS\,II}\Phi_{PS\,II}^{max} \quad (14)$$

where E_a is the absorbed excitation energy, $\Phi_{PS\,II}^{max}$ is the maximum quantum yield of PS II photochemistry, and $a_{PS\,II}$ is the *optical* absorption cross-section of PS II. Assuming that $\Phi_{PS\,II}^{max}$ can be assessed from variable fluorescence and from the extent of energy transfer between photosynthetic units [5,55], the optical absorption cross-section can be calculated from FRR measurements of $\sigma_{PS\,II}$, F_o, F_m, and p.

Under steady-state conditions ($C=1-q$=const) the rate of excitation trapping is balanced by the rate of Q_A^- reoxidation. From Eq. 3 it follows that under constant ambient light:

$$\sigma_{PS\,II}i_o\frac{q(i_o)}{(1-p)+pq(i_o)} = [1-q(i_o)]\frac{1}{\tau_{QA}(i_o)} \quad (15)$$

where i_o is the incident irradiance, $\tau_{Q_A}(i_o)$ is the irradiance-dependent, average time-constant of Q_A^- reoxidation, and $q(i_o)$ is the steady-state fraction of open RC II. Rearranging Eq. 15 we calculate $q(i_o)$ as follows:

$$q(i_o) = \frac{\sigma'_{PS\,II}(i_o)i_o}{\sigma'_{PS\,II}(i_o)i_o + \frac{1}{\tau_{Q_A}}} \quad (16)$$

where

$$\sigma'_{PS\,II}(i_o) = \frac{\sigma_{PS\,II}}{(1-p)+pq(i_o)} \quad (17)$$

reflects an increase in the functional absorption cross-section at intermediate irradiance levels due to excitation energy transfer between PS II reaction centers.

Both $\sigma_{PS\,II}$ and $a_{PS\,II}$ are wavelength-dependent; using excitation light of controlled spectral quality, the FRR technique allows measurements of the spectrally resolved functional absorption cross-section, $\sigma_{PS\,II}(\lambda)$. In this report, we limit our discussion to measurements of $\sigma_{PS\,II}$ at 475 nm, with 70 nm half-bandwidth.

2.2. Fast repetition rate fluorometry: instrumentation

The FRR instrument uses a bank of blue and green

light emitting diodes (a combination of NLPB500, 450 nm peak emission, and NSPE500, 500 nm peak emission) from Nichia, Japan, as an excitation source. To uniformly illuminate the sample chamber (a T-76 scattering cell from NSG Precision Cells, USA), three stacks of LEDs, totaling 108, are arranged as a cylinder of 64 mm diameter. Residual long-wavelength radiation from the LEDs is filtered with a cylindrical, 3-mm-thick glass filter (BG39 from Shott, Germany). The LEDs are operated at 300 mA pulsed current, and each produces ≈ 8 mW of peak optical power. To avoid thermal damage to the LEDs, the duty cycle of excitation flashes is limited to $< 5\%$. Peak optical power within the sample chamber is ≈ 0.7 W/cm^2, corresponding to a flux of 1.66×10^{22} quanta m^{-2} s^{-1} (i.e., 27 500 μmol quanta m^{-2} s^{-1}).

Emitted fluorescence is collected from the bottom of the sample chamber through a pair of interference filters (Corion S10-680-R) and a long pass filter (Shott RG665). The fluorescence signal is detected using a Hamamatsu R2066 photomultiplier operated at 300–600 V. As a reference signal, a small portion of the excitation light is detected by a Hamamatsu S1722 PIN photodiode. Both the fluorescence and the reference signals are digitized at a 16 MHz sampling rate, and transferred to a notebook computer. The digitized reference signal (*i*), and the ratio of the fluorescence to reference signal (*f*) then are analyzed with custom software in the context of Eqs. 7–9.

2.3. *Fast repetition rate fluorometry: excitation protocols*

The flexibility of the FRR protocol, which can last from tens of microseconds to seconds, permits both

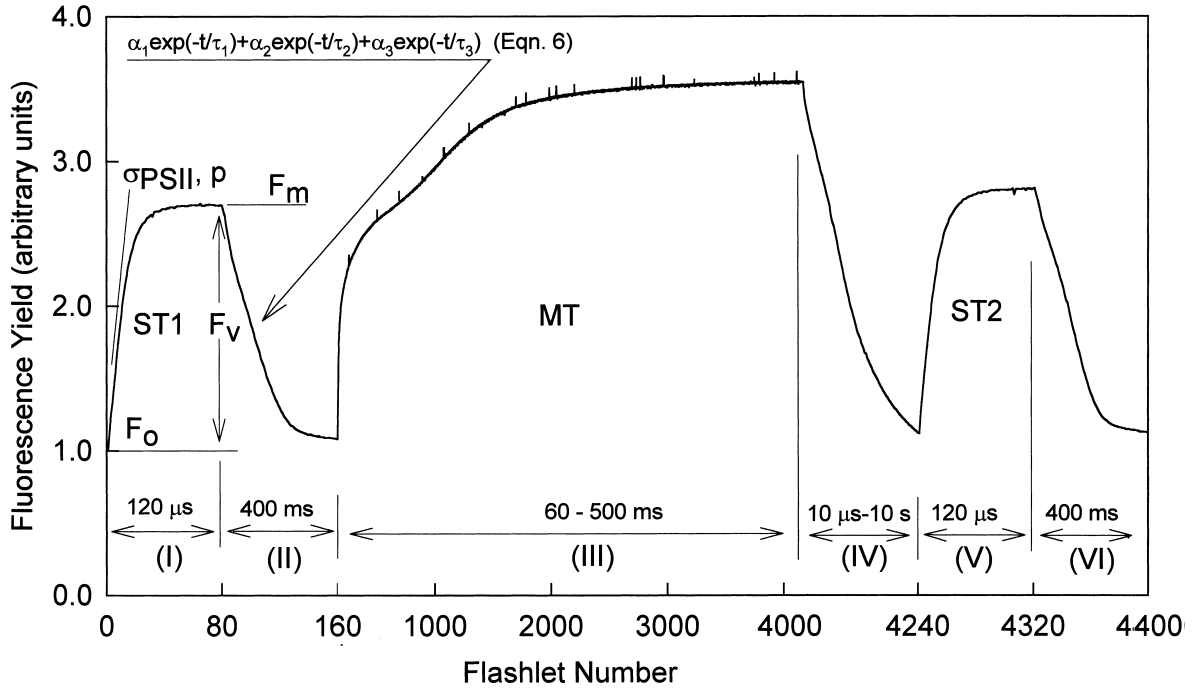

Fig. 1. Representative fluorescence transients measured by the FRR method. Phases I and V (ST flashes) are performed as a sequence of 80 to 120 flashlets of 0.125 to 1.0 μs duration, at 0.5- to 2.0-μs intervals. Phases II, IV, and VI (relaxation protocol) consist of 40 to 80 flashlets at intervals varying exponentially from 50 μs to 50 ms. Phase III (MT flash) consists of up to 4000 flashlets, at 20- to 200-μs time intervals. The length of Phase IV is varied from 1 μs to 10 s by changing the number of flashlets and time intervals between them. The fluorescence transients in Phase I and V are controlled by the F_o and F_m components of the fluorescence yield, the functional absorption cross-section ($\sigma_{PS\,II}$), and by the extent of energy transfer between PS II reaction centers, *p*. Fluorescence transients in Phases II and VI are controlled primarily by the kinetics of Q_A^- reoxidation, while the fluorescence transient in Phase IV is controlled primarily by the kinetics of PQ pool reoxidation. Phase III measures changes in fluorescence yield under multiple turnover conditions, and Phases V and VI quantify the effects of the earlier multiple turnover excitations on the photosynthetic parameters.

ST and MT excitation sequences to be executed in any combination and arbitrary delay time. During the ST protocol, high excitation energies are used to reduce Q_A within a single photochemical turnover. Operationally, the ST flash consists of a series of 80–120 flashlets, each of 0.125 to 1.0 μs duration, at 0.5 to 2.0 μs intervals, and a pulse power of $\sim$0.03 mol quanta $m^{-2} s^{-1}$ (Fig. 1, Phase I). The cumulative excitation energy during an ST flash is selected so that 3 to 4 quanta per RC II are absorbed. Inevitably, a portion of PS II reaction centers will become reoxidized and potentially can be re-reduced during the flash, thus deviating from a purely single-turnover excitation. We discuss the extent of this deviation below.

During the MT protocol, excitation energy is delivered over a longer time, allowing multiple Q_A oxidation–reduction events, and reducing the PQ pool within 60 to 500 ms. Operationally, the MT protocol consists of a sequence of up to 4000 flashlets each of 0.125 to 32 μs duration, delivered at intervals of 20 μs to 2 ms (Fig. 1, Phase III).

In addition to the ST and MT excitation flashes, the FRR protocol includes relaxation sequences to evaluate the kinetics of Q_A^- reoxidation (Eq. 6). These sequences consist of 40 to 80 low-energy flashlets at 20-μs to 50-ms intervals, and are delivered after either an ST or MT flash (Fig. 1, Phase II and IV). Usually, we follow the MT flash by a second ST/relaxation sequence at varying intervals (Fig. 1, Phase V and VI).

2.4. Experimental materials

All the results discussed in this paper are from the unicellular chlorophyte, *Chlorella pyrenoidosa*, and are representative of the FRR methodology applied to a wide variety of cultured, unicellular algae (e.g., *Dunaliella tertiolecta*, *Chlamydomonas reinhardtii*, and *Skeletonema costatum*), as well as in natural phytoplankton communities, and intact leaves from higher plants and blades of marine macrophytes. *Chlorella pyrenoidosa* was selected because it can be easily grown with minimal algal culturing facilities, making it the preferred organism to test and reproduce the methodology and results presented here.

2.5. Oxygen evolution

Oxygen flash yields were measured using a bare platinum oxygen-rate electrode as described in Ref. [37]. ST flashes for oxygen measurements were generated using a xenon flashlamp (model L21 from Hamamatsu). The flashlamp was operated in a FRR mode by applying a triggering HV pulse followed by a series of high current pulses at 1.5- to 10-μs intervals, resulting in a train of 4 to 80 flashlets delivering a total cumulative energy of 3 quanta/RC II.

3. Results

3.1. Single turnover flashes

To investigate the relationship between excitation energy and fluorescence responses, we applied an ST flash consisting of 120 flashlets of 0.2 μs to 0.8 μs duration at 1-μs intervals (Fig. 2A). With increasing excitation energies, the fluorescence yield saturates faster, reaching the F_m level within 60 μs. All the profiles displayed identical saturation kinetics as a function of cumulative excitation energy (Fig. 2B). Assuming that the steady-state fluorescence yield is controlled primarily by the ratio of the rates of Q_A reduction/reoxidation, these results suggest that, under our experimental conditions, the average time constant of Q_A^- reoxidation is much longer than the length of the flash. Hence, only a small fraction of Q_A^- is reoxidized during the flash; this fraction is independent of excitation energy. The observed fluorescence transients deviate from a cumulative one-hit Poisson distribution [13] (Fig. 2B, inset), suggesting energy transfer between PS II units. The calculated values of F_o, F_m, $\sigma_{PS\,II}$ and p are independent of excitation energy between 1.6 to 4 quanta/RC II/ST (Table 1). Although the fluorescence transients observed within 120 ms flash never reach the theoretical maximum level (Fig. 2A), the calculated *asymptotic* F_m signal is independent on the excitation energy within this range.

To further examine the effect of excitation energy on the saturation character of the fluorescence transients, we applied a series of 120 flashlets of 0.8 μs duration, but altered the intervals between them

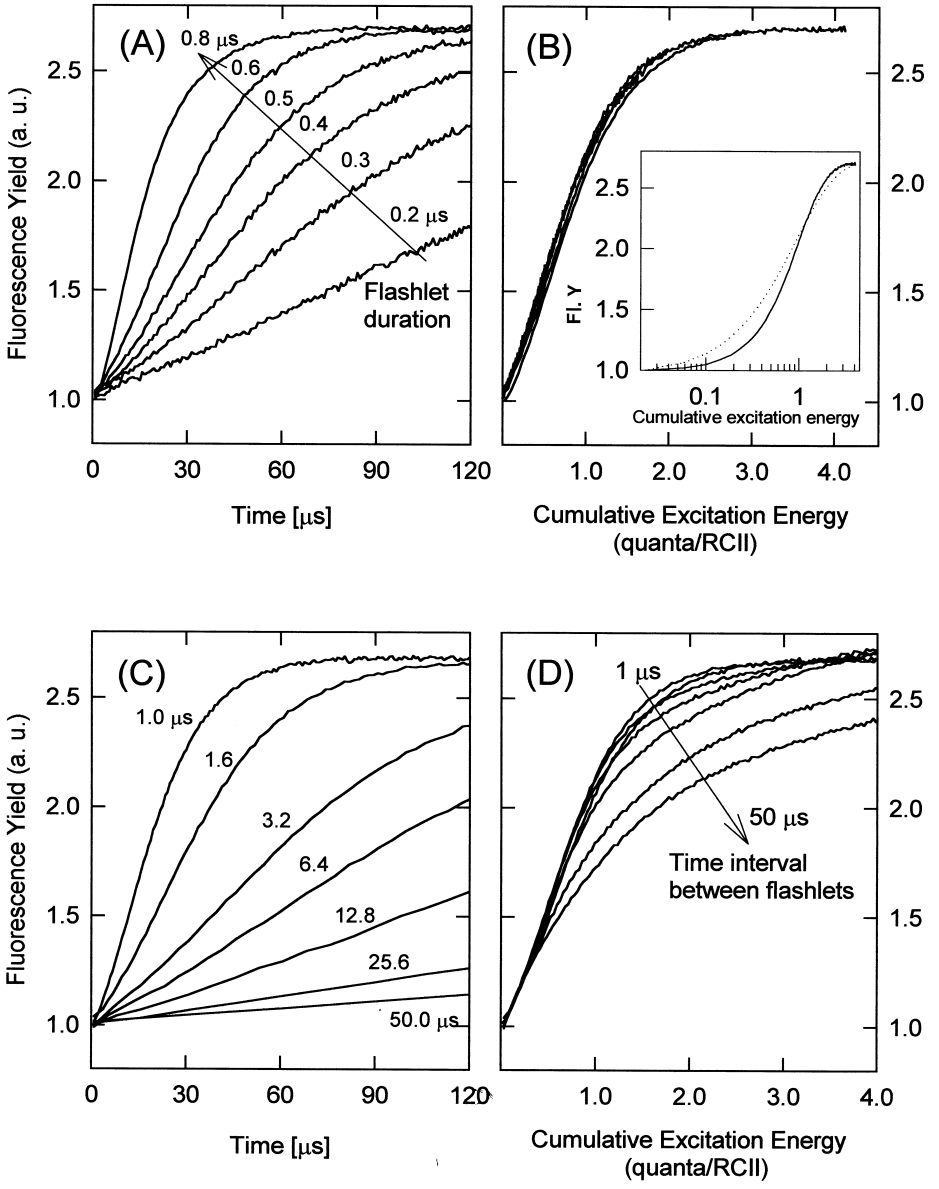

Fig. 2. Effect of excitation energy on fluorescence saturation profiles observed during an ST protocol consisting of 120 flashlets. (A) Excitation energy was controlled by varying the duration of the flashlets from 0.2 μs to 0.8 μs, while maintaining the time interval between them, at 1 μs. When plotted as a function of excitation energy (B), all the fluorescence transients displayed a similar saturation character during the 120-μs time window. Inset: an example of a fluorescence transient as a function of the log cumulative excitation energy. The solid line is experimental data, the dotted line is the fit of the data to a cumulative one-hit Poisson model assuming no energy transfer between PS II reaction centers. By neglecting energy transfer, the least squares minimization procedure forces the calculated $\sigma_{PS\,II}$ to decrease relative its correct value in order to minimize the error between the calculated and the experimental curve. (C) Excitation energy was controlled by varying the time interval between flashlets from 1 μs to 50 μs, while maintaining the length 0.8 μs. The resulting fluorescence transients showed slower saturation rates as a function of time (C), and cumulative excitation energy (D), indicating that at longer time windows the fluorescence transient is controlled by the excitation energies as well as by the rates of Q_A^- reoxidation.

from 1 μs to 50 μs (Fig. 2C). The rate of fluorescence saturation normalized to cumulative excitation energy is constant during the initial 100–200 μs (Fig. 2D). This rate declines at longer flash lengths with decreasing excitation energy, indicating an increasing effect of Q_A^- reoxidation.

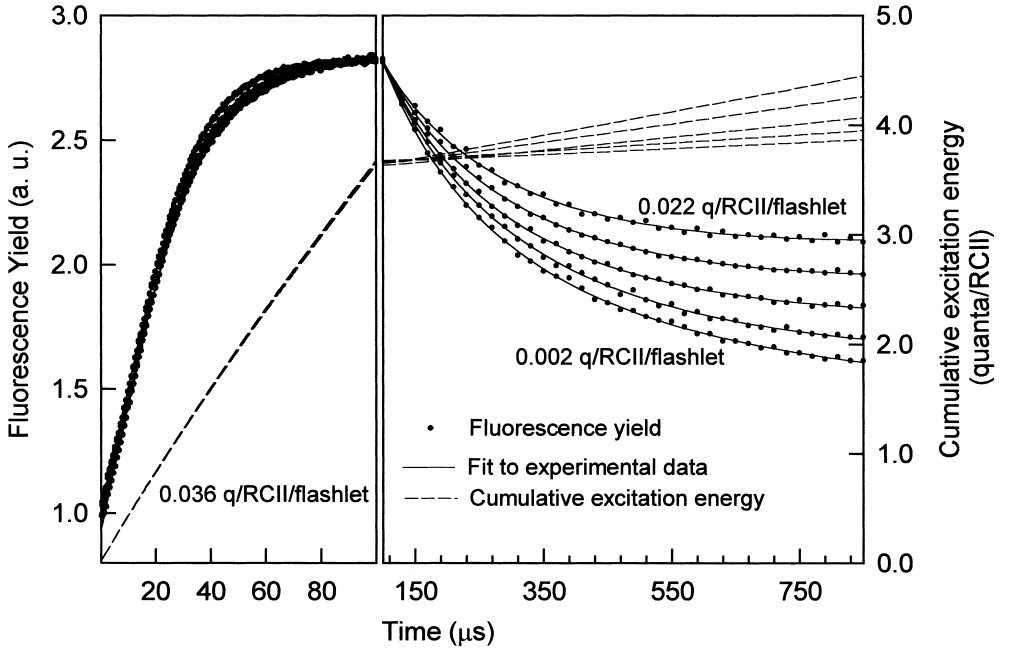

Fig. 3. FRR fluorescence transients observed during an ST flash followed by a relaxation protocol. The ST protocol consisted of 100 flashlets of 0.036 q/RC II with an interval of 1 μs. The relaxation protocol consisted of 40 flashlets at 20-μs intervals, where the excitation energy varied from 0.002 to 0.022 quanta/RC II. (●) Experimental data, (—) theoretical fit with parameters calculated as shown in Table 2. (- - -) Cumulative excitation energy.

The excitation energies selected for ST protocols are a compromise between a desire to fully reduce Q_A within a single photochemical turnover, and the desire to minimize potential non-photochemical fluorescence quenching in PS II reaction centers caused either by carotenoid triplet formation [56,57] or P_{680}^+ accumulation [8,9,52]. The latter two phenomena may reduce fluorescence yields by 20–35% during ST flashes compared with MT flashes [35]. We did not observe marked changes in F_m when the excitation intensity was decreased by a factor of three (Table 1), nor in the initial rise of fluorescence yield when the excitation intensity was decreased by a factor of 50 (Fig. 2B,D). However, F_v/F_m measured with an ST flash was approx. 0.65 in physiologically healthy algae, which is considerably lower than that of 0.75 which is sometimes observed using an MT protocol (e.g., Ref. [58]).

Table 1
Calculated values of F_o, F_m, $\sigma_{PS\,II}$, and p for single-turnover flashes with different excitation energies (Fig. 2A,B) using Eq. 8, and assuming negligible Q_A^- reoxidation during the flash

Flashlet length (μs)	Excitation energy (quanta/RC II/ST)	F_o	F_m	$\sigma_{PS\,II}$ (Å^2/q)	p
0.8	4.1	1.00	2.72	280	0.44
0.6	3.0	1.00	2.72	290	0.43
0.5	1.9	1.00	2.72	290	0.44
0.4	1.6	1.00	2.72	300	0.43
0.3	1.2	1.00	2.59	310	0.38
0.2	0.6	1.00	–	–	–

The lower limit of excitation energies to reliably calculate photosynthetic parameters is about 1.6 quanta/RC II ST under the conditions of negligible Q_A^- reoxidation. F_m values shown here are the calculated, asymptotic maximum fluorescence yield, not the fluorescence yields attained at the end of the ST flash.

3.2. FRR relaxation protocol

Following the transient reduction of Q_A by an ST flash, the decay of fluorescence is controlled by Q_A^- reoxidation kinetics [22], but is confounded by energy transfer between PS II reaction centers [59]. The kinetics of Q_A^- reoxidation can be described by a multi-exponential decay model (e.g., Eq. 6), and can be assessed with the FRR fluorometer using the described relaxation protocol. Energetically, the excitation energy used in this protocol has an actinic effect that repopulates a fraction of the reoxidized Q_A. These re-excited RC IIs display reoxidation kinetics that deviate from a single-turnover character. To investigate the effect of the relaxation protocol on the assessment of Q_A^- reoxidation kinetics, we analyzed the fluorescence responses acquired at varying excitation energies; Fig. 3 demonstrates the actinic effect of the measurement protocol. These artifacts can be minimized by using excitation protocols that produce the least actinic effect, and by numerical analysis that accounts for the inevitable re-reduction of a fraction of centers by the probe flashlets (e.g., Eqs. 8 and 9).

The kinetics of Q_A^- reoxidation calculated with such a correction (Table 2) are almost independent of the excitation energy. Deviation in the calculated parameters at the highest level of excitation energy most likely reflects changes in the population of reduced secondary electron- carriers (i.e., Q_B and PQ pool).

The cumulative energy applied during the ST portion of the excitation protocol was about 3.6 quanta/RC II, resulting in fluorescence transient from 1 to 2.84, and about 0.96 level of QA reduction at the end of the ST flash. The theoretical F_m signal calculated using Eqs. 7–9, however, was around 3.0.

3.3. Excitation energy transfer

Energy transfer between PS II reaction centers, represented by the p parameter in Eq. 1 and Eq. 5, affects both the rate of fluorescence saturation during an ST flash and fluorescence decay during relaxation protocol. As p increases, the rate at which fluorescence yields decay following the ST flash exceeds the rate of Q_A^- reoxidation. Consequently, neglecting p when analyzing the Q_A^- reoxidation underestimates the kinetic time constants, particularly the fast and medium components (last row in Table 2). Applying an arbitrary value for p may alleviate this problem [59]; however, our measurements indicate that p varies widely, and strongly depends upon the physiological condition of the cells [60]. Therefore, assessing the rates of Q_A^- reoxidation from fluorescence yield decay-curves requires calculating p on a case-by-case basis.

3.4. How 'single turnover' are ST flashes?

By definition, an ST flash induces a single photochemical event. This requirement can be evaluated by calculating the extent of Q_A^- reoxidation by Q_B during the ST flash:

$$e_t = \sum_{n=0}^{N} C_n(\alpha_1 \exp(-\Delta t_n/\tau_1) + \alpha_2 \exp(-\Delta t_n/\tau_2) + \alpha_3 \exp(-\Delta t_n/\tau_3)) \quad (18)$$

where e_t is a measure of the electron equivalents

Table 2
Fluorescence parameters and time constants of Q_A^- reoxidation for different excitation energy of the relaxation protocol (Fig. 3A,B), analyzed with the triple-exponential model of Q_A^- reoxidation, according to Eqs. 8–10

Flashlet energy q/RC II	F_o	F_m	$\sigma_{PS\ II}$ (Å^2/q)	p	α_1	τ (μs)	α_2	τ_2 (μs)	α_3	τ_3 (ms)
0.002	1.00	3.01	300	0.48	0.44	240	0.44	1240	0.12	26.9
0.004	1.00	2.99	320	0.49	0.41	250	0.44	1300	0.15	26.5
0.006	1.00	2.99	330	0.48	0.42	260	0.43	1360	0.15	26.0
0.013	1.00	2.96	310	0.45	0.40	270	0.42	1230	0.18	20.6
0.022	1.00	2.96	310	0.45	0.33	360	0.48	1280	0.21	12.4
0.002	1.00	3.00	350	0.00	0.530	180	0.380	830	0.090	29.2

The results in the last row are an example of calculations of the kinetics of Q_A^- reoxidation, neglecting energy transfer ($p = 0$).

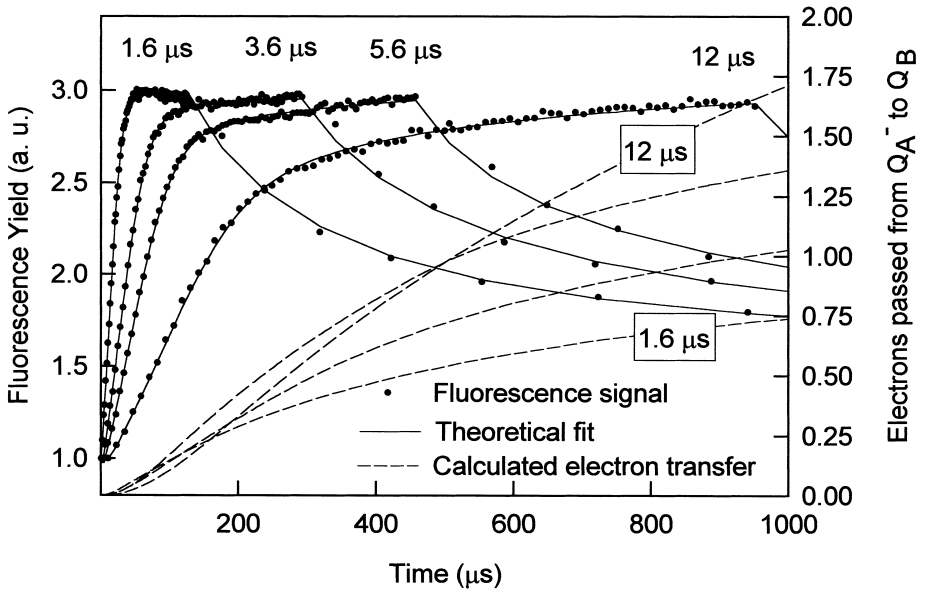

Fig. 4. Fluorescence saturation profiles and initial portion of relaxation protocol. The ST flashes consisted of a train of flashlets, applied at times varying from 1.6 µs to 12 µs (●). The relaxation kinetics were measured with flashlets applied at time intervals varied exponentially from 50 µs to 800 ms. (- - -) The calculated electron transfer from Q_A^- to secondary electron acceptors. The continuous line represents a theoretical fit to the experimental data, using Eqs. 8 and 9.

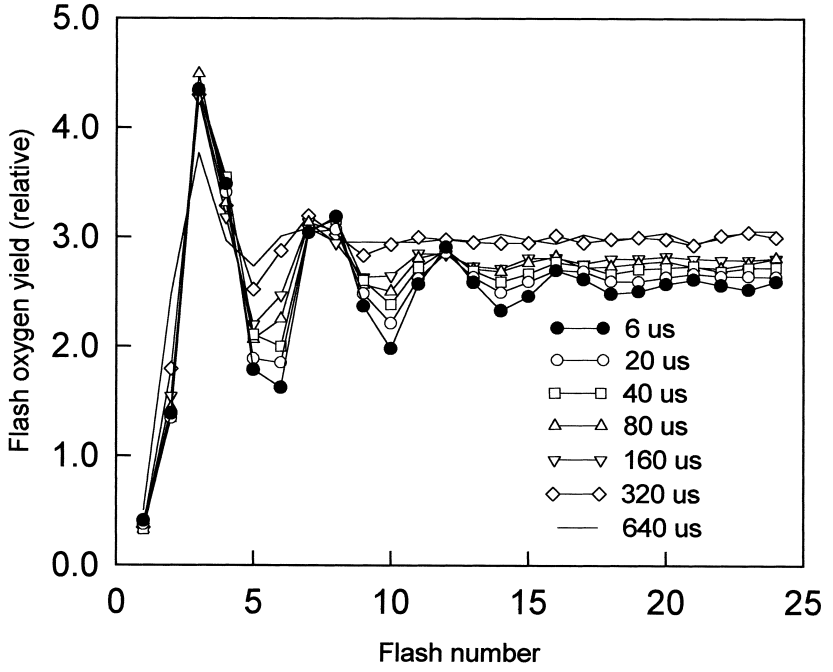

Fig. 5. Oscillation pattern of flash oxygen yields in response to a series of flashes with cumulative energy of 3 quanta/RC II and length of 6 to 640 µs, applied at 2-s time intervals. Each flash consisted of a train of 4 to 80 flashlets. The oscillatory pattern of oxygen evolution is preserved during the first four flashes of length varying from 6 to 160 µs, although its amplitude dampens with increasing flash length due to increasing probability of double-electron turnovers. The oxygen evolved during the second flash, and in the steady state (>24 flashes) increases by about 8% as the length of the flash increases from 6 µs to 80 µs, indicating $<10\%$ increase in the probability of double electron turnover during an 80-µs-long flash.

resulting from Q_A^- reoxidation occurring during N flashlets, Δt_n is the interval between flashlets, and C_n is calculated by Eq. 8. To quantify e_t we made a series of ST measurements with time intervals between flashlets varying from 1.6 μs to 12 μs, followed by a relaxation protocol (Fig. 4). From Eqs. 8 and 9, we calculate that up to 96% of PS II reaction centers were reduced within 60 μs at the highest excitation intensity, $<10\%$ of the reaction centers were reoxidized, and $<7\%$ were re-reduced by subsequent excitation during the ST flash. We conclude that the delivery of 3 to 4 excitations per RC II within 60–100 μs is effectively an ST flash. Under such conditions, $<10\%$ of the PS II reaction centers undergo multiple photochemical turnovers. As the time between flashlets was increased from 1.6 to 12 μs, the number of multiple turnovers increased by the same factor.

To independently establish the single turnover character of ST flashes, we measured oxygen flash yields using a train of flashlets with a total duration of 6 to 640 μs; these conditions were achieved using a sequence of 4 to 64 flashlets at 1.5- to 10-μs intervals, with constant cumulative excitation energy of 3 quanta/RC II. A four-flash periodicity in oxygen and fluorescence was observed, which dampened after 12 flashes (Fig. 5). Changing the length of the excitation sequence from 6 to 160 μs had little effect on the initial (first to fourth flash) oscillatory pattern for O_2 evolution (Fig. 5). The oxygen-flash yield on the second flash and in the steady-state (>24 flashes) increased by about 8% as the length of the flashes changed from 6 μs to 80 μs. We conclude that the number of double photochemical turnovers in an 80-μs-long ST flash increases by $<10\%$ when the flash length rises from 6 μs to 80 μs.

3.5. Dependence of fluorescence yield on flash number during the ST protocol

If ST flashes are applied at intervals <4 s, the fluorescence signal observed in a dark-adapted sample displays a high fluorescence yield during the first flash (HF1), followed by a weak, four-period oscillation with a lower (LF) fluorescence yield (Fig. 6) [42,61–63]. The oscillation pattern of fluorescence is generally antiparallel to that of oxygen evolution [42,64], and is absent under weak background light or in samples immediately taken from illumination to the dark. The oscillatory pattern is independent of the ST flash length in the 6–160 μs range, but dampens with longer flash durations due to multiple turnovers of PS II that randomize S-states. These results previously were interpreted as donor-side modulation of variable fluorescence [42,65]. The pattern of F_m changes in a given flash is preserved in the F_o signal on the subsequent flash (Fig. 6A), suggesting that this modulation is maintained over the lifetime of the S state (seconds) [21,24,42], rather than the lifetime of oxidized P_{680}^+ (sub-milliseconds) [66]. The modulation of the fluorescence yield by the donor side of PS II shown in Fig. 6A should *not* be confused with 'donor-side quenching' of the F_m signal [10]; the modulation reported here is preserved several seconds after an ST flash. On this time scale, potential quenchers in PS II reaction centers (e.g., P_{680}^+ and/or carotenoid triplets) have long dissipated [57,66].

When the time delay between flashes is increased to 10 s, the oscillations in fluorescence yield disappeared; however, the first flash still had a 15% to 20% higher yield than that of the second and subsequent flashes (Fig. 6B, and inset). The difference between the first and subsequent ST flashes is independent of the length of the flash in the 80–1000 μs range. When the time delay between flashes is >120 s, only the HF fluorescence yield is observed. When the sample is dark-adapted for less than 10 s, or exposed to a very weak background illumination of 0.1–0.5 μE m^{-2} s^{-1}, only the LF fluorescence yield is observed.

As the duration of the ST flash is extended beyond approx. 200 μs, the fluorescence yields decline slightly from their initial maximum. Furthermore, there is a transient spike at the onset of the relaxation sequence, indicating the development of fluorescence quenching during the excitation protocol. The extent of this quenching (3–5%), however, is much smaller than the difference between the HF and LF level.

3.6. MT flash protocol

Fluorescence transients observed during an MT flash display complicated patterns of fluorescence yield in response to progressive excitation (Fig.

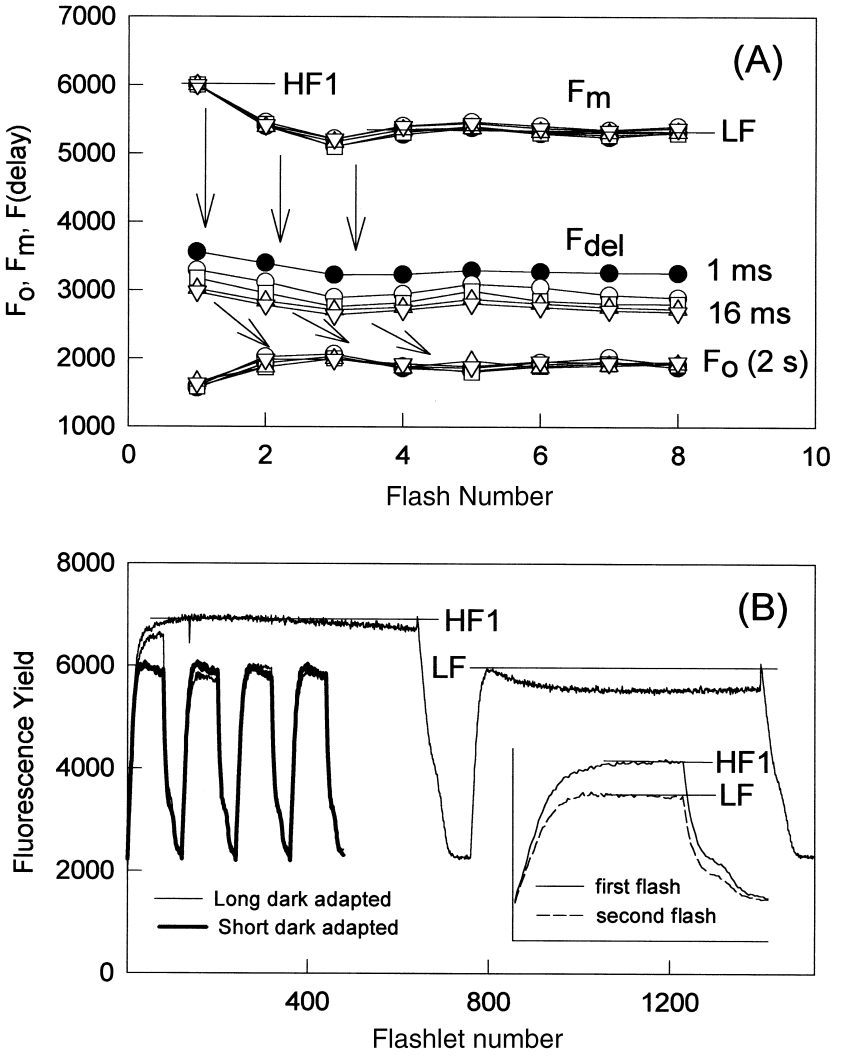

Fig. 6. ST fluorescence transient as a function of the flash number. (A) Period four oscillation of the F_m, F_o, and intermediate (F_{del}) fluorescence yield observed in a series of 100-μs-long ST flashes applied at 2-s intervals. The F_{del} fluorescence signal was measured 1 to 16 ms following the ST flash. High F_o fluorescence at given flash correlates with the high F_m fluorescence at the preceding flash. (B) Dependence of flash number of the fluorescence transient observed in a dark-adapted sample ($t_{dark} > 120$ s, thin line) and short dark-adapted sample ($t_{dark} < 10$ s, thick line). The long flashes consist of 640 flashlets of 0.8 μs duration and 1-μs intervals. Long flashes are separated by a relaxation sequence consisting of 120 flashlets applied at times exponentially increasing from 50 μs to 30 ms, over a period of 10 s. The short flashes (80 flashlets) are separated by a relaxation sequences consisting of 40 relaxation flashlets over a period of 2 s. Inset: the difference between the first and second ST flash applied on dark-adapted sample ($t_{dark} > 120$ s); high fluorescence yield (HF1) is observed during the first flash (—), and a low fluorescence yield (LF) is observed during the second and consecutive flashes (- - -).

7A). The multiphasic character of the fluorescence signal reflects sequential filling and emptying of several electron pools (Q_A, Q_B, PQ) with different reduction-oxidation rates. The expression of these phases strongly depends on the experimental protocol [67–69].

As with ST flashes, the fluorescence transients observed at the first and the second MT flash in a dark-adapted sample are very different. Fig. 7B shows representative fluorescence profiles for three pairs of MT flashes, each composed of 3000 flashlets, applied at 10-s intervals, with average excitation energies of 4000, 185, and 40 quanta/RC II/s. The first MT flash displays a higher maximal fluorescence

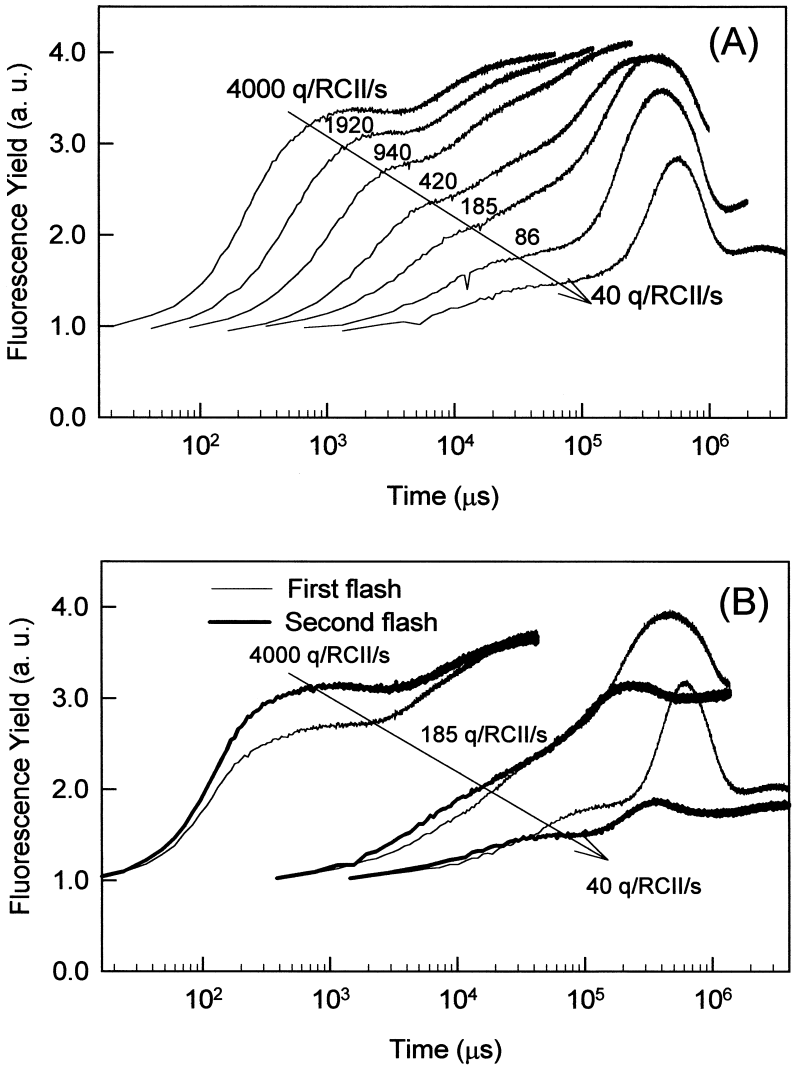

Fig. 7. Fluorescence response to multiple turnover (MT) flashes. (a) Fluorescence transients in MT flashes performed with 3000 flashlets of 0.8 μs duration and intervals varying from 20 to 2000 μs. Very high variable fluorescence ($F_v/F_m = 0.75$) is observed at excitation energies as low as 200 quanta/RC II/s. (B) Fluorescence response to a pair of MT flashes applied at 10 s delay measured in a dark-adapted sample.

yield, with a slowly saturating phase and a lower initial slope compared with subsequent ones. When the delay between flashes is longer than 2 min, the first flash response is preserved with each subsequent flash. When measured under weak background illumination or after < 10 s of dark adaptation, fluorescence yields resembled the second-flash behavior in Fig. 7B.

To further examine fluorescence responses to ST and MT flashes, we exposed cells to an ST flash (ST1) followed by an MT flash, and finally to a second ST flash (ST2), each separated by a relaxation sequence (Fig. 8A). The maximum fluorescence yield, HF2, measured during the ST2 flash depended on the interval between MT and ST2. If the ST2 flash was applied within 10 μs to 5 ms following the MT flash, the fluorescence signal remained at a level 4–5% lower than the maximum yield, HFM (Fig. 8B). As the time interval between MT and ST2 increased to 16 s, the HF2 decreased, with a time constant of approx. 4.2 s. The functional absorption cross-section measured 160 ms following MTF was about 40% lower than that measured during ST1. As the interval between MTF and ST2 in-

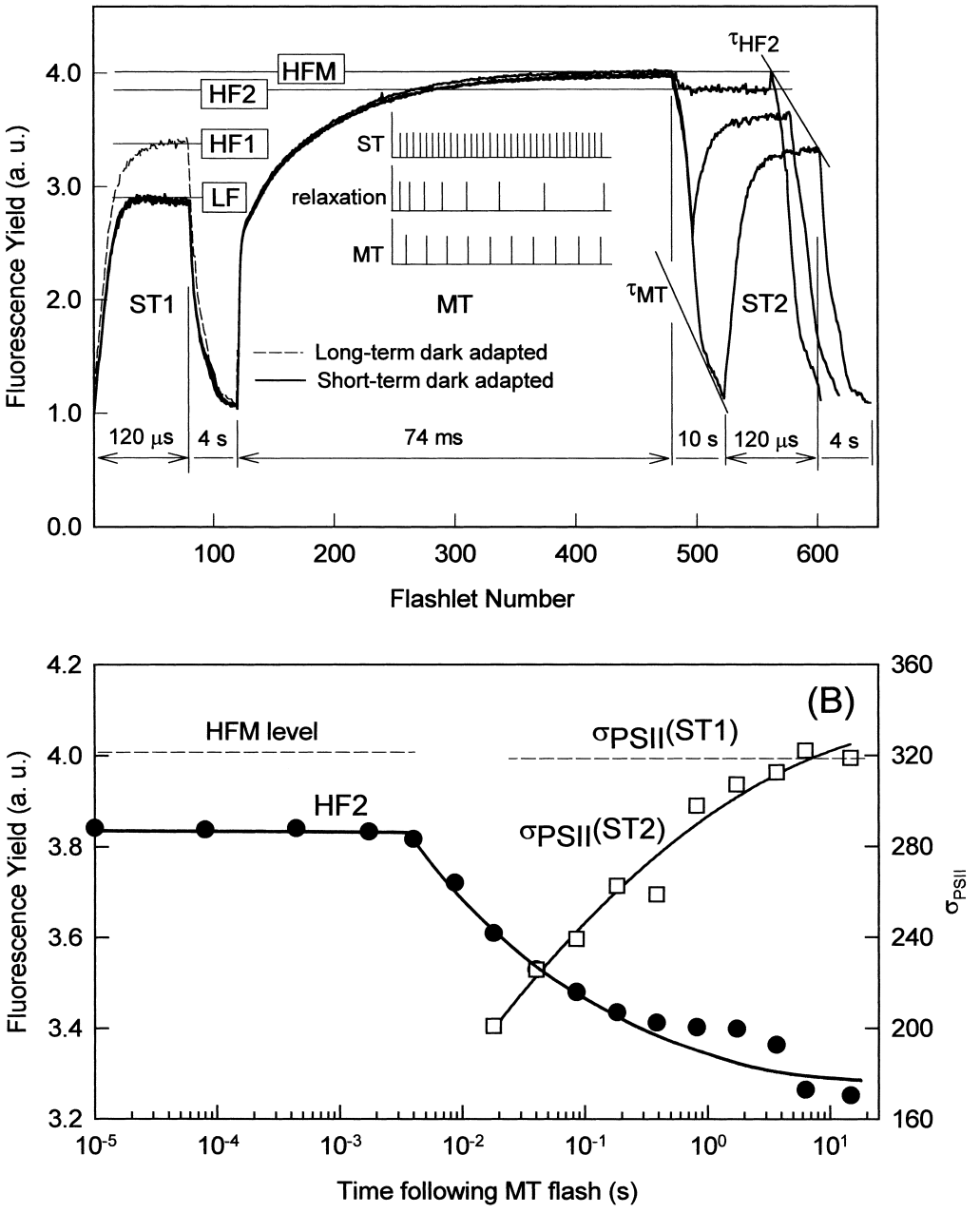

Fig. 8. (A) Fluorescence transients observed during a sequence of ST1–MT–ST2 flashes. ST flashes consist of 80 flashlets of 0.8 µs duration at 1.5-µs time interval, MT flash consists of 3200 flashlets of 0.8 µs duration or length at 20-µs intervals (every 10th flashlet in the MT flash is shown). The relaxation sequences following the ST1 and ST2 consist of 40 flashlets at intervals varying exponentially from 50 µs to 800 ms, over 4 s. Following an MT flash, the time interval between flashlets in relaxation sequence was varied from 125 µs to 2.4 s. The ST2 flash was applied 10 µs following an MT flash, at 20 ms delay, and 10 s delay. Inset: schematic representation of excitation protocol in the ST flash, relaxation sequence, and MT flash. The F_m signal observed during ST1 flash is minimal (LF) when measured on a short, dark-adapted sample ($t_{dark} < 10$ s), or in the presence of low-level background irradiance (continuous line). It increases to the HF1 level when measured on a long dark-adapted sample ($t_{dark} > 120$ s, dashed line). The F_m signal observed during the ST2 flash (HF2) approaches the level measured during a MT flash when applied immediately following a MT flash. The kinetics of F_m decrease following the MT flash ($t_{FH2} = 4.2$ s) is similar to the kinetics of the slow phase of changes in fluorescence yield following an MT flash ($t_{MT} = 2.6$ s). (B) Changes in F_m fluorescence yields and functional absorption cross-section as a function of the delay between an MT and an ST2 flash.

creased to 16 s, $\sigma_{PS\,II}$ reached the pre-MTF value, with a time constant of $\sim$1 s (Fig. 8B).

The results from the ST1–MT–ST2 protocol illustrate the differences in fluorescence yields for ST and MT measurements which are the basis of the controversy in interpreting fluorescence data [14,34, 36,51,70]. By changing the period of dark adaptation, or the time between MT and ST2, we found that the difference in F_m between MT and ST flashes was controlled primarily by the pre-illumination history, not by the intensity of excitation. The F_m signal observed during MT flash was up to 35% higher than that observed during ST flash when measured on short-term ($t_{dark} < 10$ s) dark-adapted samples. Following longer period of dark adaptation ($t_{dark} > 120$ s), this difference decreased to less than 20%. Finally, when measured shortly (10 μs to 5 ms) following the MT flash, the single-turnover F_m signal was only 5% lower than that observed during MT flash.

4. Discussion

We have presented a novel method for characterizing PS II processes based on measuring fluorescence transients in response to a series of subsaturating flashlets of controlled intensity, duration, and intervals. The key photosynthetic parameters calculated with the FRR method include $\sigma_{PS\,II}$, F_o, F_m, p, and rates of electron transport within PS II. The most controversial and protocol-dependent parameter is the maximal fluorescence level (F_m) measured upon reduction of the first electron acceptor, Q_A, commonly used in fluorescence-based models of photosynthetic yields or rates [15,28,34].

ST and MT flashes differ in their excitation intensities, durations, and the cumulative excitation energy required to induce the fluorescence responses. ST flashes are generated with excitation intensities exceeding 50000 quanta/RC II/s in <100 μs, whereas MT flashes have excitation intensities ranging from 20 to 2000 quanta/RC II/s, over a period of 50 ms to several seconds. Accordingly, the cumulative excitation-energy is 3 to 4 quanta/RC II for an ST flash, and 50 to 500 quanta/RC II for an MT flash. It has been stated that the high excitation intensity of an ST flash influences the measured fluorescence signal and prevents detection of the 'correct' fluorescence yield [10]. Our results (Fig. 8) demonstrate that the duration of the excitation protocol and total excitation energy applied, rather than excitation intensity, affects the measured fluorescence yield.

Differences in fluorescence yields for ST and MT measurements are commonly ascribed to fluorescence quenching due to over-excitation of PS II reaction centers, and resulting from accumulation of the oxidized intermediates on the donor side of PS II [8,9,52], or of carotenoid triplet states [56,57]. We attributed only 4% to 5% fluorescence quenching to either of these phenomena during extended, 640-μs-long ST protocols (Fig. 6B). This quenching is negligible during the typical 80–120-μs-long ST flashes, as demonstrated by the constant level of variable fluorescence at lower excitation energies (Fig. 2A,B). The amplitude of this quenching phenomenon cannot explain the differences between the HF and LF states. We also observed a weak, four-period oscillation in the ST fluorescence signal, which suggests that the donor side of PS II modulates the fluorescence yield somewhat (Fig. 6A). This apparent control is exerted over the lifetime of the S-states, not the lifetime of P^+_{680} (Fig. 6C), and therefore may reflect the accumulation of a positive charge near the manganese complex on the donor side of PS II [71,72]. It is possible that the difference between HF1 and LF levels (Fig. 6B) is due to a quenching by increased level of P^+_{680}, the reduction rate of which decreases during the second and subsequent flashes where the S-states become progressively scrambled. This fluorescence quenching, however, disappears immediately following the MT flash (HF2 $\cong$ HFM, Fig. 8A), where the S-states are also scrambled, indicating that the distribution of the S-states has little control over the observed quenching. The observed pattern of fluorescence modulation also can be interpreted in terms of fluorescence quenching by S-state-dependent oxygen release [73]. Within these interpretations, both the F_o and F_m signals are affected (Fig. 6A), potentially preserving the F_v/F_m or F_v/F_o ratio.

Alternatively, changes in the rate of S-state advancements may modify the lifetime of P^+_{680} following a *double* reduction of the PS II reaction center (e.g., when reduction of P^+_{680} requires prior advancement of S-states). The probability of double reduction during an ST flash may reach 5% to 10% depending on

the experimental conditions, potentially resulting in a long-lived, weak four-period oscillation during a sequence of ST flashes [62,74,75]. The transient decline in fluorescence induced by 640-μs-long, high-intensity flashes (Fig. 6B), or with an ST flash applied immediately after an MT flash (Fig. 8) might be explained by double hits leading to an accumulation of P_{680}^{+}. Within this model, the F_m signal would be preferentially quenched, causing a decrease in the F_v/F_m ratio. The amplitude of this effect ($\sim$5%), however, is negligible in comparison to the difference between ST and MT fluorescence yields (up to 35%). We conclude that the comparatively high excitation intensity used in the ST flash protocol cannot induce the observed difference in fluorescence yields between ST and MT flashes. Consequently, such differences in fluorescence yields are due either to changes in the rate of excitation trapping by the reaction centers, and/or result from processes on the acceptor side of PS II.

The differences in F_m observed in ST and MT flashes affect assessments of the photosynthetic quantum yields based on calculating F_v/F_m [5], and so apparently underestimate Φ_{PSII}^{max} based on ST measurements [34]. As shown in Eq. 14, $\sigma_{PS\,II}$ can be expressed as the product of Φ_{PSII}^{max} and the optical absorption cross-section of PS II. The FRR fluorescence technique described here can determine $\sigma_{PS\,II}$ instantaneously (within approx. 100 μs). The decrease in $\sigma_{PS\,II}$ observed in the HF2 state (Fig. 8B) suggests that Φ_{PSII}^{max} *decreases* as the fluorescence yield increases during MT protocols. Our results suggest that the redox state on the acceptor side affects the distribution of excitation energy between photochemistry and fluorescence. The simultaneous rise in fluorescence yield and decrease in $\sigma_{PS\,II}$ suggests that the rates of radiative deactivation increase at the cost of photochemistry. An antiparallel relationship between the rates of oxygen evolution and slow phases of fluorescence induction is well documented [38,76,77], and a parallel relationship between oxygen flash yields and $\sigma_{PS\,II}$ was observed [37]. These observations are consistent with our findings.

In conclusion, the FRR methodology discussed here allows exhaustive characterization of PS II fluorescence under conditions of either ST or MT excitation. Using FRR fluorescence in conjunction with molecular genetic approaches and other biophysical techniques, we can examine the processes controlling variations in the fluorescence yields and develop a model to account for these variations [53].

Acknowledgements

We dedicate this paper to David Mauzerall from Rockefeller University for his counsel and guidance through the years. We thank Dr. Michael Behrenfeld for his valuable comments on the manuscript, and Kevin Wyman for his technical assistance. This research was supported by the U.S. Department of Energy under Contract No. DE-AC02-76CH0000016, and the Office of Naval Research under Grant 97PR00617-00.

References

[1] P.G. Falkowski, Z. Kolber, Variations in chlorophyll fluorescence yields in phytoplankton in the world oceans, Aust. J. Plant Physiol. 22 (1995) 341–355.
[2] G.H. Krause, E. Weis, Chlorophyll fluorescence and photosynthesis – the basics, Annu. Rev. Plant Physiol. Plant Mol. Biol. 42 (1991) 313–349.
[3] W.L. Butler, M. Kitajima, Energy transfer between PSII and PSI in chloroplasts, Biochim. Biophys. Acta 396 (1975) 72–85.
[4] E. Weis, J.A. Berry, Quantum efficiency of photosystem II in relation to 'energy' – quenching of chlorophyll fluorescence, Biochim. Biophys. Acta 894 (1990) 198–208.
[5] B. Genty, J.M. Briantias, N.R. Baker, The relationship between the quantum yield of photosynthetic electron transport and quenching of chlorophyll fluorescence, Biochim. Biophys. Acta 990 (1989) 87–92.
[6] S. Malkin, B. Kok, Fluorescence induction studies in isolated chloroplastsI. Number of components involved in the reaction and quantum yields,, Biochim. Biophys. Acta 126 (1966) 413–432.
[7] N. Murata, M. Nishimura, A. Takamiya, Fluorescence of chlorophyll in photosynthetic systemsII. Induction of fluorescence in isolated spinach chloroplasts,, Biochim. Biophys. Acta 120 (1966) 23–33.
[8] W.L. Butler, On the primary nature of fluorescence yield changes associated with photosynthesis, Proc. Natl. Acad. Sci. U.S.A. 69 (1972) 3420–3422.
[9] A. Sonneveld, H. Rademaker, L.N.M. Duysens, Chlorophyll a fluorescence as a monitor of nanosecond reduction of the photooxidized primary donor P_{680}^{+} of Photosystem II, Biochim. Biophys. Acta 548 (1979) 536–551.
[10] U. Schreiber, C. Neubauer, The polyphasic rise of chlorophyll fluorescence upon onset of strong continuous illumina-

tionII. Partial control by the photosystem II donor side and possible ways of interpretation,, Z. Naturforsch. 42c (1987) 1255–1264.
[11] C. Bonaventura, J. Myers, Fluorescence and oxygen evolution from *Chlorella pyrenoidosa*, Biochim. Biophys. Acta 189 (1969) 366–383.
[12] D.C. Mauzerall, Multiple excitation and the yield of chlorophyll a fluorescence in photosynthetic system, Photochem. Photobiol. 28 (1978) 991–998.
[13] A.C. Ley, D.C. Mauzerall, Absolute absorption cross-sections for photosystem II and the minimum quantum requirement for photosynthesis in *Chlorella vulgaris*, Biochim. Biophys. Acta 680 (1982) 95–106.
[14] P.G. Falkowski, K. Wyman, A.C. Ley, D.C. Mauzerall, Relationship of steady-state photosynthesis to fluorescence in eucaryotic algae, Biochim. Biophys. Acta 849 (1986) 183–192.
[15] B. Genty, J. Harbinson, J.M. Briantais, N.R. Baker, The relationship between non-photochemical quenching of chlorophyll fluorescence and the rate of photosystem II photochemistry in leaves, Photosynth. Res. 25 (1990) 249–257.
[16] G. Samson, D. Bruce, Complementary changes in absorption cross-sections of photosystems-I and photosystems-II due to phosphorylation and Mg^{2+} depletion in spinach thylakoids, Biochim. Biophys. Acta 1232 (1995) 21–26.
[17] G. Paillotin, Capture frequency excitation and energy transfer between photosynthetic units in the Photosystem II, J. Theor. Biol. 58 (1976) 219–235.
[18] A.C. Ley, D.C. Mauzerall, The extent of energy transfer among Photosystem II reaction centers in *Chlorella*, Biochim. Biophys. Acta 850 (1986) 234–248.
[19] B. Bouges-Bocquet, Electron transfer between the two photosystems in spinach chloroplasts, Biochim. Biophys. Acta 314 (1973) 250–256.
[20] B. Diner, Dependence of the turnover and deactivation reactions of Photosystem II on the redox state of the pool A varied under anaerobic conditions, in: Proceedings of the Third International Congress on Photosynthesis II, Elsevier, Amsterdam, 1974, pp. 589–601.
[21] J. Bowes, A.R. Crofts, Binary oscillations in the rate of reoxidation of the primary acceptor of Photosystem II, Biochim. Biophys. Acta 590 (1980) 373–384.
[22] A.R. Crofts, C.A. Wraight, The electrochemical domain of photosynthesis, Biochim. Biophys. Acta 726 (1983) 149–185.
[23] H.H. Robinson, A.R. Crofts, Kinetics of the oxidation-reduction reactions of the photosystem II quinone acceptor complex, and the pathway for deactivation, FEBS Lett. 153 (1983) 221–226.
[24] D.M. Kramer, H.R. Robinson, A.R. Crofts, A portable multi-flash kinetic fluorimeter for measurement of donor and acceptor reactions of photosystem 2 in leaves of intact plants under field conditions, Photosynth. Res. 26 (1990) 181–193.
[25] P.G. Falkowski, Z. Kolber, Y. Fujita, Effect of redox state on the dynamics of photosystem II during steady-state photosynthesis in eucaryotic algae, Biochim. Biophys. Acta 933 (1988) 432–443.
[26] J. Lavergne, H.W. Trissl, Theory of fluorescence induction in photosystem II: derivation of analytical expressions in a model including exciton-Radical pair equilibrium and restricted energy transfer between photosynthetic units, Biophys. J. 68 (1995) 2474–2492.
[27] Z. Kolber, J. Zehr, P. Falkowski, Effects of growth irradiance and nitrogen limitation on photosynthetic energy conversion in photosystem II, Plant Physiol. 88 (1988) 923–929.
[28] Z. Kolber, P.G. Falkowski, Use of active fluorescence to estimate phytoplankton photosynthesis in situ, Limnol. Oceanogr. 38 (1993) 1646–1665.
[29] A.R. Crofts, C.T. Yerkes, A molecular mechanism for qE-quenching, FEBS Lett. 352 (1994) 265–270.
[30] L.L. France, N.E. Geacintov, J. Breton, L. Valkunas, The dependence of the degrees of sigmoidicities of fluorescence induction curves in spinach chloroplasts on the duration of actinic pulses in Pump-Probe experiments, Biochim. Biophys. Acta 1101 (1992) 105–119.
[31] H.W. Trissl, Y. Gao, K. Wulf, Theoretical fluorescence induction curves derived from coupled differential equations describing the primary photochemistry of photosystem-II by an exciton radical pair equilibrium, Biophys. J. 64 (1993) 984–998.
[32] A.R. Holzwarth, Is it time to throw away your apparatus for chlorophyll fluorescence induction?, Biophys. J. 64 (1993) 1280–1281.
[33] P.G. Falkowski, Z. Kolber, D.C. Mauzerall, A comment on the call to throw away your fluorescence induction apparatus, Biophys. J. 66 (1994) 923–925.
[34] U. Schreiber, H. Hormann, C. Neubauer, C. Klughammer, Assessment of photosystem-II photochemical quantum yield by chlorophyll fluorescence quenching analysis, Aust. J. Plant Physiol. 22 (1995) 209–220.
[35] U. Schreiber, A. Krieger, Two fundamentally different types of variable chlorophyll fluorescence in-vivo, FEBS Lett. 397 (1996) 131–135.
[36] G. Samson, D. Bruce, Origins of the low-yield of chlorophyll a fluorescence induced by single turnover flash in spinach thylakoids, Biochim. Biophys. Acta 1276 (1996) 147–153.
[37] O. Prasil, Z. Kolber, J.A. Berry, P.G. Falkowski, Cyclic electron flow around photosystem-II in-vivo, Photosynth. Res. 48 (1996) 395–410.
[38] H. Kautsky, A. Hirsh, Neue Versuche zur Kohlensauerassimilation, Naturwissenschaften 48 (1931) 964.
[39] Govindjee, Sixty-three years since Kautsky: chlorophyll *a* fluorescence, Aust. J. Plant Physiol. 22 (1995) 131–160.
[40] M. Bradbury, N.R. Baker, A quantitative determination of photochemical and non-photochemical quenching during the slow phase of the chlorophyll fluorescence induction curve of bean leaves, Biochim. Biophys. Acta 765 (1984) 275–281.
[41] U. Schreiber, U. Schliwa, W. Bilger, Continuous recording of photochemical and non-photochemical chlorophyll fluorescence quenching with a new type of modulation fluorometer, Photosynth. Res. 10 (1986) 51–62.

[42] R. Delosme, New results about chlorophyll fluorescence in vivo, in: G. Forti, A. Melandri (Eds.), Proceedings of the 2nd International Congress on Photosynthesis, W. Junk Publishers, The Hague, 1971, pp. 187–195.
[43] D.C. Mauzerall, Light-induced changes in Chlorella and the primary photoreaction for the production of oxygen, Proc. Natl. Acad. Sci. U.S.A. 69 (1972) 1358–1362.
[44] J.R. Flemming, Chemical Applications of Ultrafast Spectroscopy, Oxford University Press, New York, 1986.
[45] A. Joliot, Effect of low temperature (−30 to −60°C) on the reoxidation of the photosystem II primary electron transport in the presence and absence of 3(3,4-dichlorphenyl)-1,1-dimethylurea, Biochim. Biophys. Acta 357 (1974) 439–448.
[46] P.G. Falkowski, Y. Fujita, A. Ley, D.C. Mauzerall, Evidence for cyclic electron flow around Photosystem II in *Chlorella pyrenoidosa*, Plant Physiol. 81 (1986) 310–312.
[47] Z.G. Cerovic, M. Bergher, Y. Goulas, S. Tosti, I. Moya, Simultaneous measurement of changes in red and blue fluorescence in illuminated isolated chloroplasts and leaf pieces – the contribution of NADPH to the blue fluorescence signal, Photosynth. Res. 36 (1993) 193–204.
[48] D.M. Kramer, A.R. Crofts, Control and measurement of photosynthetic electron transport in vivo, in: N. Baker (Ed.), Photosynthesis and the Environment, Kluwer Academic, Dordrecht, The Netherlands, 1996, pp. 25–66.
[49] M. Trtilek, M. Koblizek, L. Nedbal, Dual-modulation LED kinetic fluorometer, J. Luminesc. 72-74 (1997) 597.
[50] B. Diner, Dependence of the deactivation reactions of Photosystem II on the redox state of plastoquinone pool A varied under anaerobic conditions. Equilibria on the acceptor side of Photosystem II, Biochim. Biophys. Acta 460 (1977) 247–258.
[51] M.D. Kramer, G. DiMarco, F. Loreto, Contribution of plastoquinone quenching to saturation pulse-induced rise of chlorophyll fluorescence in leaves, in: P. Mathis (Ed.), Photosynthesis: From Light to Biosphere, vol. I, Kluwer Academic, Dordrecht, The Netherlands, 1995, pp. 147–150.
[52] G. Deprez, A. Dobek, N.E. Geacintov, G. Paillotin, J. Breton, Probing florescence induction in chloroplasts on a nanosecond time scale utilizing picosecond laser pulse pair, Biochim. Biophys. Acta 752 (1983) 444–454.
[53] A. Prasil, Z.S. Kolber, P.G. Falkowski, Measurements of variable chlorophyll fluorescence using fast repetition rate techniques. Modulation of quantum yields by the QB binding site, Photosynth. Res. (1998) submitted.
[54] G. Paillotin, Movement of excitations in the photosynthetic domains of Photosystem II, J. Theor. Biol. 58 (1976) 237–252.
[55] H.W. Trissl, J. Lavergne, Fluorescence induction from photosystem II: Analytical equations for the yields of photochemistry and fluorescence derived from analysis of model including exciton-radical pair equilibrium and restricted energy transfer between photosynthetic units., Aust. J. Plant Physiol. 22 (1995) 183–193.
[56] J. Breton, N.E. Geacintov, C.E. Swenberg, Quenching of fluorescence by triplet excited states in chloroplasts, Biochim. Biophys. Acta 548 (1979) 616–635.
[57] A. Sonnenveld, H. Rademaker, L.N.M. Duysens, Transfer and trapping of excitation energy in Photosystem II as studied by chlorophyll a fluorescence quenching by dinitrobenzene and carotenoid triplet. The matrix model, Biochim. Biophys. Acta 593 (1980) 272–289.
[58] C. Geel, Photosystem II electron flow as a measure for phytoplankton gross primary production, Ph.D. Thesis, Department of Plant Physiology, Wageningen Agricultural University, Wageningen, 1997.
[59] J.J. Eaton-Rye, Govindjee, Electron transfer through the quinone acceptor complex of photosystem II in bicarbonate-depleted spinach thylakoid membranes as a function of actinic flash number and frequency, Biochim. Biophys. Acta 935 (1988) 237–247.
[60] I.R. Vassiliev, Z.S. Kolber, D. Mauzerall, V.K. Shukla, K. Wyman, P.G. Falkowski, Effects of iron limitation on photosystem II composition and energy trapping in *Dunaliella tertiolecta*, Plant Physiol. 109 (1995) 963–972.
[61] P. Joliot, A. Joliot, B. Bouges, G. Barbieri, Studies of photosystem II photocenters by comparative measurements of luminescence, fluorescence and oxygen emission, Photochem Photobiol. 14 (1971) 287–305.
[62] H. Robinson, A.R. Crofts, Kinetics of the changes in the oxidation-reduction state of the acceptors and donors of photosystem II in pea thylakoids measured by flash fluorescence, in: J. Biggins (Ed.), Progress in Photosynthesis, vol. II, Martinus Nijhoff, Dordrecht, 1987, pp. 429–432.
[63] D.M. Kramer, A.R. Crofts, Demonstration of a highly-sensitive portable double-flash kinetic spectrophotometer for measurement of electron transfer reactions in intact plants, Photosynth. Res. 23 (1990) 231–240.
[64] M.J. Delrieu, F. Rosengard, Fundamental differences between period-4 oscillations of the oxygen and fluorescence yield induced by flash excitation in inside-out thylakoids, Biochim. Biophys. Acta 892 (1987) 163–171.
[65] P. Joliot, A. Joliot, Different types of quenching involved in photosystem II centers, Biochim. Biophys. Acta 305 (1973) 302–316.
[66] K. Brettel, E. Shlodder, H.T. Witt, Nanosecond reduction kinetics of photooxidized chlorophyll-aII (P-680) in single flashes as a probe for the electron pathway, H^+-release, and charge accumulation in the O_2 evolving complex, Biochim. Biophys. Acta 766 (1984) 403–415.
[67] C. Neubauer, U. Schreiber, The polyphasic rise of chlorophyll fluorescence upon onset of strong continuous illuminationI. Saturation characteristics and partial control by the photosystem II acceptor side,, Z Naturforsch c 42 (1987) 1246–1254.
[68] R.J. Strasser, A. Srivastava, Govindjee, Polyphasic chlorophyll-a fluorescence transients in plants and cyanobacteria, Photochem. Photobiol. 61 (1995) 32–42.
[69] A. Srivastava, R.J. Strasser, Govindjee, Polyphasic rise of chlorophyll-a fluorescence in herbicide-resistant D1 mutants

of *Chlamydomonas reinhardtii*, Photosynth. Res. 43 (1995) 131–141.
[70] C. Vernotte, A.L. Etienne, J.M. Briantais, Quenching of the system II chlorophyll fluorescence by the plastoquinone pool, Biochim. Biophys. Acta 545 (1979) 519–527.
[71] M.J. Delrieu, F. Rosengard, Events near the reaction center in O-2 evolving PS-II enriched thylakoid membranes – The presence of an electric field during the S-2 state in a population of centers, Photosynth. Res. 37 (1993) 205–215.
[72] A. Boussac, J.J. Girerd, A.W. Rutherford, Conversion of the spin-state of the manganese complex in photosystem-II induced by near-infrared light, Biochemistry 35 (1996) 6984–6989.
[73] V.P. Shinkarev, X. Chunhe, Govindjee, C.A. Wraight, Kinetics of the oxygen evolution step in plants determined from flash-induced chlorophyll a fluorescence, Photosynth. Res. 51 (1997) 43–49.
[74] V.P. Shinkarev, C.A. Wraight, Kinetic factors in the bicycle model of oxygen evolution by photosystem II, Photosynth. Res. 38 (1993) 315–321.
[75] V.P. Shinkarev, C. Xu, Govindjee, C.A. Wraight, Kinetics of the oxygen evolution step in situ estimated from its quenching effects on flash-induced chlorophyll a fluorescence, Biophys. J. 66 (1994) A114.
[76] E.D. MacAlister, J. Myers, The time course of photosynthesis and fluorescence observed simultaneously, Smithsonian Institution Publications Miscellaneous Collections 99 (1940) 1–37.
[77] W.P. Quick, H. Horton, Studies on the induction of chlorophyll fluorescence in barley chloroplastsI. Factors affecting the observations of oscillation in the yield of chlorophyll fluorescence and the rate of oxygen evolution,, Proc. R. Soc. Lond. B 220 (1984) 361–370.